# Constraining gluon PDFs with quarkonium production


Melih A. Ozcelik

Institut de Physique Nucléaire Orsay/Université Paris-Sud

*ozcelik@ipno.in2p3.fr*

Collaborators: M.G. Echevarria, J.-P. Lansberg, C. Pisano, A. Signori


*LightCone 2019 - Ecole Polytechnique*
16-20 September 2019

# Quarkonia & PDFs: Phenomenology

# the $\eta_c$ - a good gluon probe

- $\eta_c$ is a gluon probe at low scales

# the $\eta_c$ - a good gluon probe

- $\eta_c$ is a gluon probe at low scales
- simplest of all quarkonia as far as computation of hadro-production

# the $\eta_c$ - a good gluon probe

- $\eta_c$ is a gluon probe at low scales
- simplest of all quarkonia as far as computation of hadro-production
- $\eta_c$ cross section computation known

# the $\eta_c$ - a good gluon probe

- $\eta_c$ is a gluon probe at low scales
- simplest of all quarkonia as far as computation of hadro-production
- $\eta_c$ cross section computation known
  - at NLO since 1992 in collinear factorisation

**[J. Kühn, E. Mirkes, Phys.Lett. B296 (1992) 425-429]**

# the $\eta_c$ - a good gluon probe

- $\eta_c$ is a gluon probe at low scales
- simplest of all quarkonia as far as computation of hadro-production
- $\eta_c$ cross section computation known
  - at NLO since 1992 in collinear factorisation

    **[J. Kühn, E. Mirkes, Phys.Lett. B296 (1992) 425-429]**
  - at LO since 2012 and at NLO since 2013 in TMD factorisation

    **[D. Boer, C. Pisano, Phys.Rev. D86 (2012) 094007]**

    **[J.P. Ma, J.X. Wang, S. Zhao, Phys.Rev. D88 (2013) no.1, 014027]**

# the $\eta_c$ - a good gluon probe

- $\eta_c$ is a gluon probe at low scales
- simplest of all quarkonia as far as computation of hadro-production
- $\eta_c$ cross section computation known
  - at NLO since 1992 in collinear factorisation

    **[J. Kühn, E. Mirkes, Phys.Lett. B296 (1992) 425-429]**
  - at LO since 2012 and at NLO since 2013 in TMD factorisation

    **[D. Boer, C. Pisano, Phys.Rev. D86 (2012) 094007]**

    **[J.P. Ma, J.X. Wang, S. Zhao, Phys.Rev. D88 (2013) no.1, 014027]**
- first hadro-production measurement data released in 2015 by LHCb ($p_T > 6$ GeV) **[LHCb, Eur.Phys.J. C75 (2015) no.7, 311.]**

# $\eta_c$ data at LHCb - 2015

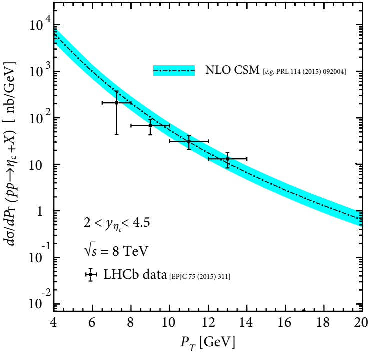


**[M. Butenschoen, Z.-G. He, and B.A. Kniehl, PRL 114 (2015) 092004]**
**[H. Han, Y.-Q. Ma, C. Meng, H.-S. Shao and K.-T. Chao, PRL 114 (2015) 092005]**
**[H.-F. Zhang, Z. Sun, W.-L. Sang and R. Li, PRL 114 (2015) 092006]**

- first hadro-production measurement data released in 2014 by LHCb ($p_T > 6$ GeV) **[LHCb, Eur.Phys.J. C75 (2015) no.7, 311.]**

# $\eta_c$ data at LHCb - 2015

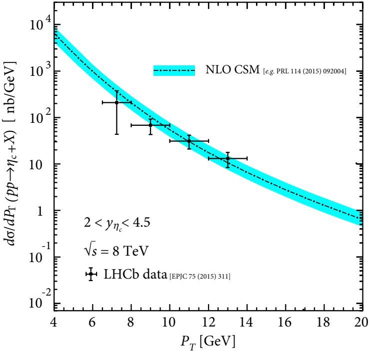


- first hadro-production measurement data released in 2014 by LHCb ($p_T > 6$ GeV) **[LHCb, Eur.Phys.J. C75 (2015) no.7, 311.]**
  - NLO Colour-Singlet Model describes LHCb data well (see plot)

# $\eta_c$ data at LHCb - 2015

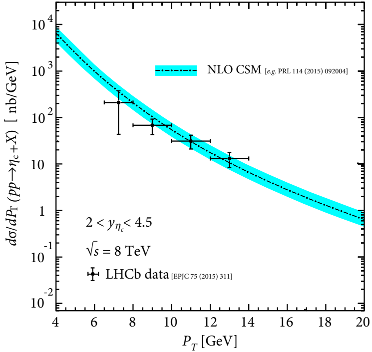


- first hadro-production measurement data released in 2014 by LHCb ($p_T > 6$ GeV) **[LHCb, Eur.Phys.J. C75 (2015) no.7, 311.]**
  - NLO Colour-Singlet Model describes LHCb data well (see plot)
  - unfortunately, data do not cover low $p_T$, however could be measured down to $p_T = 0$ at fixed-target experiment AFTER

**[C. Hadjidakis et al., arXiv:1807.00603 [hep-ex]]**
**[Y. Feng et al., Nucl.Phys. B945 (2019) 114662]**

# the $\eta_c$ - a good gluon probe

- $\eta_c$ is a gluon probe at low scales
- simplest of all quarkonia as far as computation of hadro-production
- $\eta_c$ cross section computation known
  - at NLO since 1992 in collinear factorisation
  - at LO since 2012 and at NLO since 2013 in TMD factorisation
- first hadro-production measurement data released in 2014 by LHCb ($p_T > 6$ GeV)
  - NLO Colour-Singlet Model describes LHCb data well (see plot)
  - unfortunately, data do not cover low $p_T$, however could be measured down to $p_T = 0$ at fixed-target experiment AFTER
- encounter problem of *negative* cross-sections with $\eta_c$ and other quarkonium bound states

# the $\eta_c$ - a good gluon probe

- $\eta_c$ is a gluon probe at low scales
- simplest of all quarkonia as far as computation of hadro-production
- $\eta_c$ cross section computation known
  - at NLO since 1992 in collinear factorisation
  - at LO since 2012 and at NLO since 2013 in TMD factorisation
- first hadro-production measurement data released in 2014 by LHCb ($p_T > 6$ GeV)
  - NLO Colour-Singlet Model describes LHCb data well (see plot)
  - unfortunately, data do not cover low $p_T$, however could be measured down to $p_T = 0$ at fixed-target experiment AFTER
- encounter problem of *negative* cross-sections with $\eta_c$ and other quarkonium bound states
- how to resolve the issue with *negative* cross-sections?

# the $\eta_c$ - a good gluon probe

- $\eta_c$ is a gluon probe at low scales
- simplest of all quarkonia as far as computation of hadro-production
- $\eta_c$ cross section computation known
  - at NLO since 1992 in collinear factorisation
  - at LO since 2012 and at NLO since 2013 in TMD factorisation
- first hadro-production measurement data released in 2014 by LHCb ($p_T > 6$ GeV)
  - NLO Colour-Singlet Model describes LHCb data well (see plot)
  - unfortunately, data do not cover low $p_T$, however could be measured down to $p_T = 0$ at fixed-target experiment AFTER
- encounter problem of *negative* cross-sections with $\eta_c$ and other quarkonium bound states
- how to resolve the issue with *negative* cross-sections?

  $\rightarrow$ how is this related to PDFs?

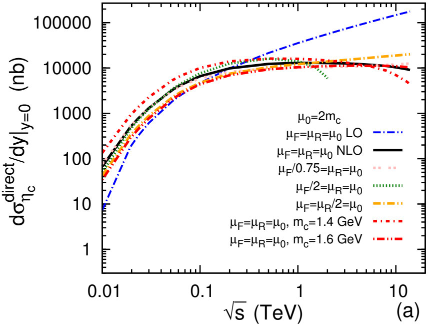


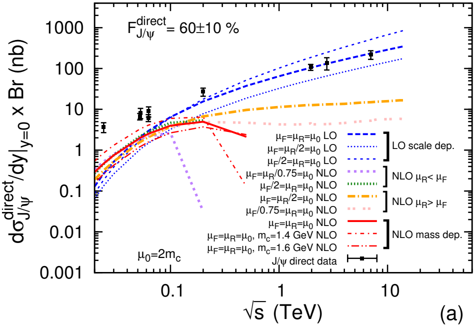


comparison of $\eta_c$ (left) and $J/\psi$ (right) differential cross-sections at NLO with different scale choices of $\mu_R$ and $\mu_F$ with CTEQ6M

**[Y. Feng, J.-P. Lansberg, J.X. Wang, Eur.Phys.J. C75 (2015) no.7, 313]**

# negative cross-sections - sources?

- What are the potential sources for negative cross-sections?:

# negative cross-sections - sources?

- What are the potential sources for negative cross-sections?:
  - is it due to a failure of theoretical models (NRQCD etc.) for quarkonia?

# negative cross-sections - sources?

- What are the potential sources for negative cross-sections?:
  - is it due to a failure of theoretical models (NRQCD etc.) for quarkonia?
  - is it due to the truncation of fixed-order calculations? Do we need to go to higher orders (N2LO, N3LO, ...) to solve the issue of negative cross-sections?

# negative cross-sections - sources?

- What are the potential sources for negative cross-sections?:
  - is it due to a failure of theoretical models (NRQCD etc.) for quarkonia?
  - is it due to the truncation of fixed-order calculations? Do we need to go to higher orders (N2LO, N3LO, ...) to solve the issue of negative cross-sections?
  - is it due to collinear factorisation? Do we need to include TMD effects?

# negative cross-sections - open $c\bar{c}$ production at N2LO

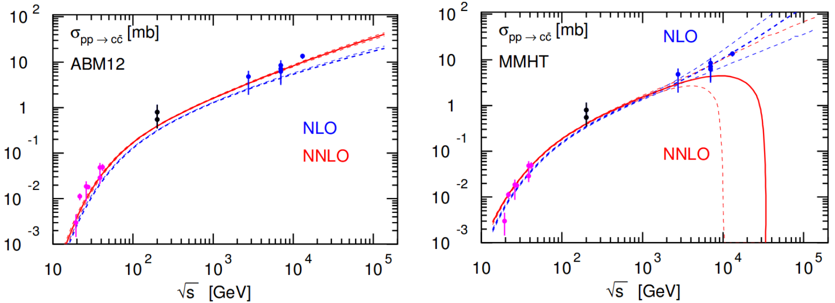


open $c\bar{c}$ production at NLO/N2LO, comparison with different PDFs (ABM12, MMHT) **[Accardi et al., Eur.Phys.J. C76 (2016) no.8, 471]**

in this case, people attribute the negative cross-section to negative gluon PDFs at low scales and rather low-$x$, however

# negative cross-sections - open $c\bar{c}$ production at N2LO

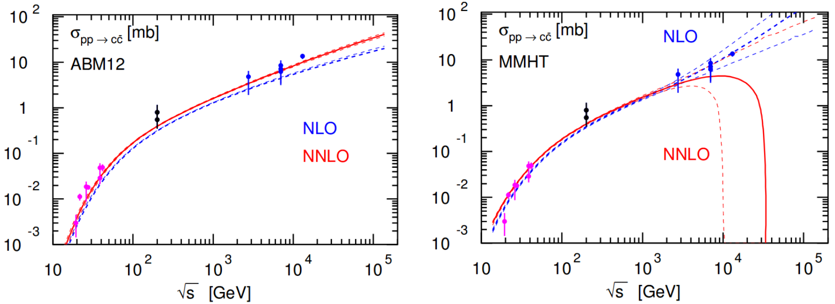


open $c\bar{c}$ production at NLO/N2LO, comparison with different PDFs (ABM12, MMHT) **[Accardi et al., Eur.Phys.J. C76 (2016) no.8, 471]**

in this case, people attribute the negative cross-section to negative gluon PDFs at low scales and rather low-$x$, however

- $\frac{d\sigma}{dy}$ does not exist at NNLO

# negative cross-sections - open $c\bar{c}$ production at N2LO

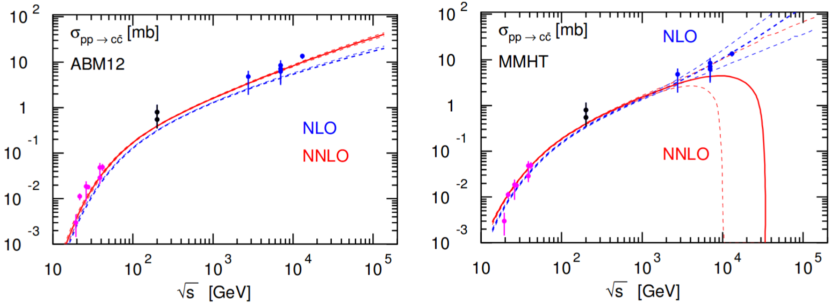


open $c\bar{c}$ production at NLO/N2LO, comparison with different PDFs (ABM12, MMHT) **[Accardi et al., Eur.Phys.J. C76 (2016) no.8, 471]**

in this case, people attribute the negative cross-section to negative gluon PDFs at low scales and rather low-$x$, however

- $\frac{d\sigma}{dy}$ does not exist at NNLO
- full scale analysis not yet performed

# negative cross-sections - open $c\bar{c}$ production at N2LO

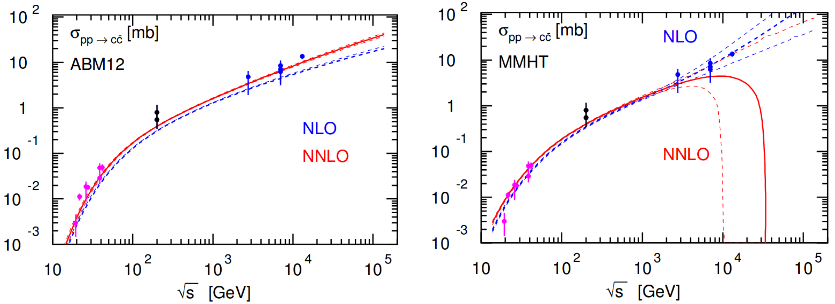


open $c\bar{c}$ production at NLO/N2LO, comparison with different PDFs (ABM12, MMHT) **[Accardi et al., Eur.Phys.J. C76 (2016) no.8, 471]**

in this case, people attribute the negative cross-section to negative gluon PDFs at low scales and rather low-$x$, however

- $\frac{d\sigma}{dy}$ does not exist at NNLO
- full scale analysis not yet performed
  $\rightarrow$ therefore one cannot rule out the possibility of negative cross-sections with positive PDFs

# negative cross-sections - open $c\bar{c}$ production at N2LO

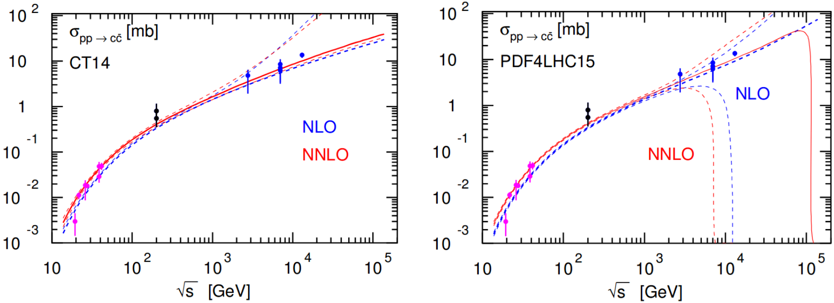


open $c\bar{c}$ production at NLO/N2LO, comparison with different PDFs (CT14, PDF4LHC15) **[Accardi et al., Eur.Phys.J. C76 (2016) no.8, 471]**

# negative cross-sections - sources?

- What are the potential sources for negative cross-sections?:
  - ~~is it due to a failure of theoretical models (NRQCD etc.) for quarkonia?~~ $\rightarrow$ No, it is a more general problem; see open $c\bar{c}$ production
  - ~~is it due to the truncation of fixed-order calculations? Do we need to go to higher orders (N2LO, N3LO, ...) to solve the issue of negative cross-sections?~~ $\rightarrow$ No, the situation at higher orders will be worse; see open $c\bar{c}$ production
  - is it due to collinear factorisation? Do we need to include TMD effects?

# negative cross-sections - sources?

- What are the potential sources for negative cross-sections?:
  - ~~is it due to a failure of theoretical models (NRQCD etc.) for quarkonia?~~ $\rightarrow$ No, it is a more general problem; see open $c\bar{c}$ production
  - ~~is it due to the truncation of fixed-order calculations? Do we need to go to higher orders (N2LO, N3LO, ...) to solve the issue of negative cross-sections?~~ $\rightarrow$ No, the situation at higher orders will be worse; see open $c\bar{c}$ production
  - is it due to collinear factorisation? Do we need to include TMD effects? (see TMD side)
  - is it due to unfortunate choices of renormalisation $\mu_R$ and factorisation $\mu_F$ scales?

# negative cross-sections - sources?

- What are the potential sources for negative cross-sections?:
  - ~~is it due to a failure of theoretical models (NRQCD etc.) for quarkonia?~~ $\rightarrow$ No, it is a more general problem; see open $c\bar{c}$ production
  - ~~is it due to the truncation of fixed-order calculations? Do we need to go to higher orders (N2LO, N3LO, ...) to solve the issue of negative cross-sections?~~ $\rightarrow$ No, the situation at higher orders will be worse; see open $c\bar{c}$ production
  - is it due to collinear factorisation? Do we need to include TMD effects? (see TMD side)
  - is it due to unfortunate choices of renormalisation $\mu_R$ and factorisation $\mu_F$ scales?
  - or is it due to Parton Distribution Functions (PDFs)?

# collinear factorisation - $\eta_c$ at NLO - hadronic cross-section

process

$$p + p \to \eta_c + X \tag{1}$$

hadronic cross-section

$$\sigma_{pp} = \sum_{ij} \int dx_1 dx_2 \; f_{i/p}(x_1, \mu_F) f_{j/p}(x_2, \mu_F) \; \hat{\sigma}_{ij}(\mu_R, \mu_F, x_1, x_2, \hat{s} = s\, x_1 x_2) \tag{2}$$

hadronic cross-section has dependence on the scales $(\mu_R, \mu_F, s)$

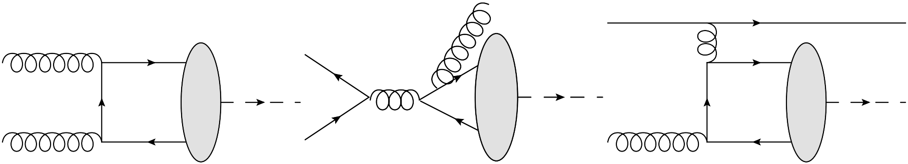

three channels contributing to $\eta_c$ production at NLO; left - $gg$ channel, middle - $q\bar{q}$ channel, right - $qg$ channel

# $\eta_c$ at NLO - historical development

- J. Kühn & E. Mirkes compute pseudo-scalar toponium cross-section at NLO in 1992 **[J. Kühn, E. Mirkes, Phys.Lett. B296 (1992) 425-429]**

# $\eta_c$ at NLO - historical development

- J. Kühn & E. Mirkes compute pseudo-scalar toponium cross-section at NLO in 1992 **[J. Kühn, E. Mirkes, Phys.Lett. B296 (1992) 425-429]**
- G. Schuler publishes his Review in 1994 **[G. Schuler, arXiv:hep-ph/9403387]**

# $\eta_c$ at NLO - historical development

- J. Kühn & E. Mirkes compute pseudo-scalar toponium cross-section at NLO in 1992 **[J. Kühn, E. Mirkes, Phys.Lett. B296 (1992) 425-429]**
- G. Schuler publishes his Review in 1994 **[G. Schuler, arXiv:hep-ph/9403387]**
  - confirms result by J. Kühn & E. Mirkes

# $\eta_c$ at NLO - historical development

- J. Kühn & E. Mirkes compute pseudo-scalar toponium cross-section at NLO in 1992 **[J. Kühn, E. Mirkes, Phys.Lett. B296 (1992) 425-429]**
- G. Schuler publishes his Review in 1994 **[G. Schuler, arXiv:hep-ph/9403387]**
  - confirms result by J. Kühn & E. Mirkes
  - points out issues with negative cross-sections at high energies

# $\eta_c$ at NLO - historical development

- J. Kühn & E. Mirkes compute pseudo-scalar toponium cross-section at NLO in 1992 **[J. Kühn, E. Mirkes, Phys.Lett. B296 (1992) 425-429]**
- G. Schuler publishes his Review in 1994 **[G. Schuler, arXiv:hep-ph/9403387]**
  - confirms result by J. Kühn & E. Mirkes
  - points out issues with negative cross-sections at high energies
  - demonstrates that for some PDF choices there is strong/weak scale dependence

# $\eta_c$ at NLO - historical development

- J. Kühn & E. Mirkes compute pseudo-scalar toponium cross-section at NLO in 1992 **[J. Kühn, E. Mirkes, Phys.Lett. B296 (1992) 425-429]**
- G. Schuler publishes his Review in 1994 **[G. Schuler, arXiv:hep-ph/9403387]**
  - confirms result by J. Kühn & E. Mirkes
  - points out issues with negative cross-sections at high energies
  - demonstrates that for some PDF choices there is strong/weak scale dependence
- M. Mangano comes to same conclusions as G. Schuler in his 1996 Proceedings **[M.L. Mangano, A. Petrelli, Int.J.Mod.Phys. A12 (1997) 3887-3897]**

# $\eta_c$ at NLO - historical development

- J. Kühn & E. Mirkes compute pseudo-scalar toponium cross-section at NLO in 1992 **[J. Kühn, E. Mirkes, Phys.Lett. B296 (1992) 425-429]**
- G. Schuler publishes his Review in 1994 **[G. Schuler, arXiv:hep-ph/9403387]**
  - confirms result by J. Kühn & E. Mirkes
  - points out issues with negative cross-sections at high energies
  - demonstrates that for some PDF choices there is strong/weak scale dependence
- M. Mangano comes to same conclusions as G. Schuler in his 1996 Proceedings **[M.L. Mangano, A. Petrelli, Int.J.Mod.Phys. A12 (1997) 3887-3897]**
- A. Petrelli *et al.* confirm result by J. Kühn & E. Mirkes in 1997 **[A. Petrelli et al., Nucl.Phys. B514 (1998) 245-309]**

# $\eta_c$ at NLO - historical development

- J. Kühn & E. Mirkes compute pseudo-scalar toponium cross-section at NLO in 1992 **[J. Kühn, E. Mirkes, Phys.Lett. B296 (1992) 425-429]**
- G. Schuler publishes his Review in 1994 **[G. Schuler, arXiv:hep-ph/9403387]**
  - confirms result by J. Kühn & E. Mirkes
  - points out issues with negative cross-sections at high energies
  - demonstrates that for some PDF choices there is strong/weak scale dependence
- M. Mangano comes to same conclusions as G. Schuler in his 1996 Proceedings **[M.L. Mangano, A. Petrelli, Int.J.Mod.Phys. A12 (1997) 3887-3897]**
- A. Petrelli *et al.* confirm result by J. Kühn & E. Mirkes in 1997 **[A. Petrelli et al., Nucl.Phys. B514 (1998) 245-309]**
- I confirm that everybody above was correct ;-)

# Schuler 1994 - Review

- appearance of negative cross-sections for quarkonia at high energies

# Schuler 1994 - Review

- appearance of negative cross-sections for quarkonia at high energies
- Schuler identifies two potential sources

# Schuler 1994 - Review

- appearance of negative cross-sections for quarkonia at high energies
- Schuler identifies two potential sources
    - small $x$-behaviour of gluon and sea-quark distributions

# Schuler 1994 - Review

- appearance of negative cross-sections for quarkonia at high energies
- Schuler identifies two potential sources
    - small $x$-behaviour of gluon and sea-quark distributions
    - behaviour of partonic cross-sections away from threshold

# Mangano 1996 - Proceedings

¶Most of the remarks which follow have already been made by G. Schuler in his '94 review [9]. Schuler at the time had available the full NLO corrections to $\eta$ production, as well as the leading small-$x$ behaviour of the $\chi$ cross sections. It is a pity that those remarks have passed almost unnoticed in the community!

**[M.L. Mangano, A. Petrelli, Int.J.Mod.Phys. A12 (1997) 3887-3897]**

# Mangano 1996 - Proceedings

¶Most of the remarks which follow have already been made by G. Schuler in his '94 review [9]. Schuler at the time had available the full NLO corrections to $\eta$ production, as well as the leading small-$x$ behaviour of the $\chi$ cross sections. It is a pity that those remarks have passed almost unnoticed in the community!

**[M.L. Mangano, A. Petrelli, Int.J.Mod.Phys. A12 (1997) 3887-3897]**

- arrives to similar conclusions that steeper gluon PDF choices will give better results because real corrections become less relevant (see Schuler's table) at high hadronic energies

# Mangano 1996 - Proceedings

¶Most of the remarks which follow have already been made by G. Schuler in his '94 review [9]. Schuler at the time had available the full NLO corrections to $\eta$ production, as well as the leading small-$x$ behaviour of the $\chi$ cross sections. It is a pity that those remarks have passed almost unnoticed in the community!

**[M.L. Mangano, A. Petrelli, Int.J.Mod.Phys. A12 (1997) 3887-3897]**

- arrives to similar conclusions that steeper gluon PDF choices will give better results because real corrections become less relevant (see Schuler's table) at high hadronic energies
- confirms that partonic high-energy limit has the general structure,

$$\lim_{z\to 0} \hat{\sigma}_{gg} = 2C_A \frac{\alpha_s}{\pi} \hat{\sigma}_{\mathrm{Born}} \left( \log \frac{M^2}{\mu_F^2} - C_J \right), \tag{3}$$

$$\lim_{z\to 0} \hat{\sigma}_{qg} = C_F \frac{\alpha_s}{\pi} \hat{\sigma}_{\mathrm{Born}} \left( \log \frac{M^2}{\mu_F^2} - C_J \right), \tag{4}$$

where $C_J$ is a process-dependent quantity

# $\eta_c$ - factorisation scale $\mu_F$

- default scale choice is $\mu_R = \mu_F = 2m_c = 3\text{GeV}$

# $\eta_c$ - factorisation scale $\mu_F$

- default scale choice is $\mu_R = \mu_F = 2m_c = 3\text{GeV}$
- most PDFs are parametrised at a scale close to the mass of the charm quark $\rightarrow$ there is only little evolution of DGLAP equations $\rightarrow$ PDFs will therefore strongly depend on the input of the initial parametrisation **[M.L. Mangano, A. Petrelli, Int.J.Mod.Phys. A12 (1997) 3887-3897]**

# $\eta_c$ - factorisation scale $\mu_F$

- default scale choice is $\mu_R = \mu_F = 2m_c = 3\text{GeV}$
- most PDFs are parametrised at a scale close to the mass of the charm quark $\rightarrow$ there is only little evolution of DGLAP equations $\rightarrow$ PDFs will therefore strongly depend on the input of the initial parametrisation **[M.L. Mangano, A. Petrelli, Int.J.Mod.Phys. A12 (1997) 3887-3897]**
- let's make a comparison with $\eta_b$, why do we not encounter negative cross-sections?

# $\eta_c$ versus $\eta_b$

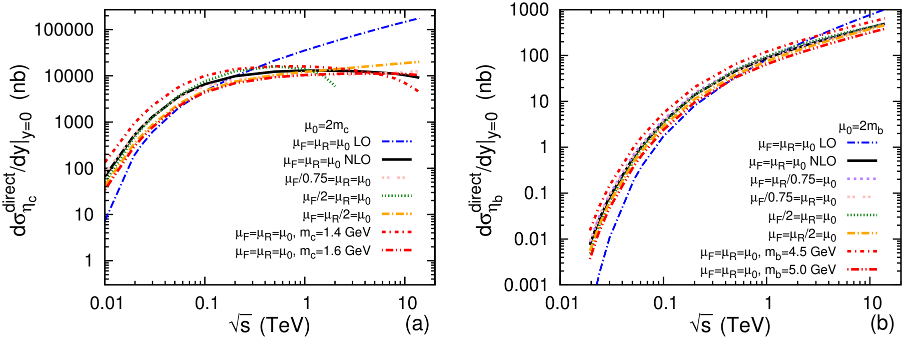


comparison of $\eta_b$ differential cross-section at NLO with different choices of $\mu_R$ and $\mu_F$ with CTEQ6M **[Y. Feng, J.-P. Lansberg, J.X. Wang, Eur.Phys.J. C75 (2015) no.7, 313]**

# $\eta_c$ versus $\eta_b$

- $\eta_b$ differential cross-section is much more stable than in case of $\eta_c$. The NLO result is the same for both particles. With only the mass increasing from $m_c$ to $m_b$, we can describe three effects:

# $\eta_c$ versus $\eta_b$

- $\eta_b$ differential cross-section is much more stable than in case of $\eta_c$. The NLO result is the same for both particles. With only the mass increasing from $m_c$ to $m_b$, we can describe three effects:
  - the dependence of the cross-section on $\sqrt{s}$ is now stretched out by the ratio the mass changed

# $\eta_c$ versus $\eta_b$

- $\eta_b$ differential cross-section is much more stable than in case of $\eta_c$. The NLO result is the same for both particles. With only the mass increasing from $m_c$ to $m_b$, we can describe three effects:
  - the dependence of the cross-section on $\sqrt{s}$ is now stretched out by the ratio the mass changed
  - the rescaling of strong coupling constant $\alpha_s$; higher scales mean lower coupling $\rightarrow$ QCD corrections become weaker, hence the NLO cross-section will be closer to LO

# $\eta_c$ versus $\eta_b$

- $\eta_b$ differential cross-section is much more stable than in case of $\eta_c$. The NLO result is the same for both particles. With only the mass increasing from $m_c$ to $m_b$, we can describe three effects:
  - the dependence of the cross-section on $\sqrt{s}$ is now stretched out by the ratio the mass changed
  - the rescaling of strong coupling constant $\alpha_s$; higher scales mean lower coupling $\rightarrow$ QCD corrections become weaker, hence the NLO cross-section will be closer to LO
  - the third effect is evolution of the PDFs from the scale of $\eta_c$ to $\eta_b$. Evolution leads to steeper gluon PDFs, hence real corrections are further surpressed

# $\eta_c$ versus $\eta_b$

- $\eta_b$ differential cross-section is much more stable than in case of $\eta_c$. The NLO result is the same for both particles. With only the mass increasing from $m_c$ to $m_b$, we can describe three effects:
  - the dependence of the cross-section on $\sqrt{s}$ is now stretched out by the ratio the mass changed
  - the rescaling of strong coupling constant $\alpha_s$; higher scales mean lower coupling $\rightarrow$ QCD corrections become weaker, hence the NLO cross-section will be closer to LO
  - the third effect is evolution of the PDFs from the scale of $\eta_c$ to $\eta_b$. Evolution leads to steeper gluon PDFs, hence real corrections are further surpressed

    $\rightarrow$ **essentially ensuring the positivity of the $\eta_b$ cross-section**

# $\eta_c$ versus $\eta_b$

- $\eta_b$ differential cross-section is much more stable than in case of $\eta_c$. The NLO result is the same for both particles. With only the mass increasing from $m_c$ to $m_b$, we can describe three effects:
  - the dependence of the cross-section on $\sqrt{s}$ is now stretched out by the ratio the mass changed
  - the rescaling of strong coupling constant $\alpha_s$; higher scales mean lower coupling $\rightarrow$ QCD corrections become weaker, hence the NLO cross-section will be closer to LO
  - the third effect is evolution of the PDFs from the scale of $\eta_c$ to $\eta_b$. Evolution leads to steeper gluon PDFs, hence real corrections are further surpressed

    $\rightarrow$ **essentially ensuring the positivity of the $\eta_b$ cross-section**
  - note however that the NLO result start to deviate from LO at large $\sqrt{s}$

# negative cross-sections - sources?

- What are the potential sources for negative cross-sections?:
  - ~~is it due to a failure of theoretical models (NRQCD etc.) for quarkonia?~~ $\rightarrow$ No, it is a more general problem; see open $c\bar{c}$ production
  - ~~is it due to the truncation of fixed-order calculations? Do we need to go to higher orders (N2LO, N3LO, ...) to solve the issue of negative cross-sections?~~ $\rightarrow$ No, the situation at higher orders will be worse; see open $c\bar{c}$ production
  - is it due to collinear factorisation? Do we need to include TMD effects? (see TMD side)
  - ~~is it due to unfortunate choices of renormalisation $\mu_R$ and factorisation $\mu_F$ scales?~~ $\rightarrow$ No, since the $\eta_c$ is a low scale process, it depends crucially on the PDF parametrisation; no physical reason to go to artificially large scales
  - or is it due to Parton Distribution Functions (PDFs)?

# negative cross-sections - sources?

- What are the potential sources for negative cross-sections?:
  - ~~is it due to a failure of theoretical models (NRQCD etc.) for quarkonia?~~ $\rightarrow$ No, it is a more general problem; see open $c\bar{c}$ production
  - ~~is it due to the truncation of fixed-order calculations? Do we need to go to higher orders (N2LO, N3LO, ...) to solve the issue of negative cross-sections?~~ $\rightarrow$ No, the situation at higher orders will be worse; see open $c\bar{c}$ production
  - is it due to collinear factorisation? Do we need to include TMD effects? (see TMD side)
  - ~~is it due to unfortunate choices of renormalisation $\mu_R$ and factorisation $\mu_F$ scales?~~ $\rightarrow$ No, since the $\eta_c$ is a low scale process, it depends crucially on the PDF parametrisation; no physical reason to go to artificially large scales
  - **or is it due to Parton Distribution Functions (PDFs)?**

# Quarkonia & PDFs: Results

# PDF parametrisation

- as pointed out by Schuler and Mangano, different PDF parametrisations can give very different result

# PDF parametrisation

- as pointed out by Schuler and Mangano, different PDF parametrisations can give very different result
- we will put this into practice and compute the K-factor for 5 different PDF choices at $y=0$. We will plot the energy-dependence of the K-factor for the PDFs:

# PDF parametrisation

- as pointed out by Schuler and Mangano, different PDF parametrisations can give very different result
- we will put this into practice and compute the K-factor for 5 different PDF choices at y=0. We will plot the energy-dependence of the K-factor for the PDFs:
  - CT14nlo_NF3

# PDF parametrisation

- as pointed out by Schuler and Mangano, different PDF parametrisations can give very different result
- we will put this into practice and compute the K-factor for 5 different PDF choices at y=0. We will plot the energy-dependence of the K-factor for the PDFs:
  - CT14nlo_NF3
  - NNPDF31sx_nlo_as_0118

# PDF parametrisation

- as pointed out by Schuler and Mangano, different PDF parametrisations can give very different result
- we will put this into practice and compute the K-factor for 5 different PDF choices at y=0. We will plot the energy-dependence of the K-factor for the PDFs:
    - CT14nlo_NF3
    - NNPDF31sx_nlo_as_0118
    - NNPDF31sx_nlonllx_as_0118

# PDF parametrisation

- as pointed out by Schuler and Mangano, different PDF parametrisations can give very different result
- we will put this into practice and compute the K-factor for 5 different PDF choices at y=0. We will plot the energy-dependence of the K-factor for the PDFs:
  - CT14nlo_NF3
  - NNPDF31sx_nlo_as_0118
  - NNPDF31sx_nlonllx_as_0118
  - MRS(A')

# PDF parametrisation

- as pointed out by Schuler and Mangano, different PDF parametrisations can give very different result
- we will put this into practice and compute the K-factor for 5 different PDF choices at y=0. We will plot the energy-dependence of the K-factor for the PDFs:
  - CT14nlo_NF3
  - NNPDF31sx_nlo_as_0118
  - NNPDF31sx_nlonllx_as_0118
  - MRS(A')
  - MRS(G)

# PDF parametrisation

- as pointed out by Schuler and Mangano, different PDF parametrisations can give very different result
- we will put this into practice and compute the K-factor for 5 different PDF choices at y=0. We will plot the energy-dependence of the K-factor for the PDFs:
  - CT14nlo_NF3
  - NNPDF31sx_nlo_as_0118
  - NNPDF31sx_nlonllx_as_0118
  - MRS(A')
  - MRS(G)
- in order to discriminate between the PDF choices we will use two different scale configurations:

# PDF parametrisation

- as pointed out by Schuler and Mangano, different PDF parametrisations can give very different result
- we will put this into practice and compute the K-factor for 5 different PDF choices at y=0. We will plot the energy-dependence of the K-factor for the PDFs:
  - CT14nlo_NF3
  - NNPDF31sx_nlo_as_0118
  - NNPDF31sx_nlonllx_as_0118
  - MRS(A')
  - MRS(G)
- in order to discriminate between the PDF choices we will use two different scale configurations:
  - $\mu_R = \mu_F = 2m_c = 3\text{GeV}$ - default scale choice

# PDF parametrisation

- as pointed out by Schuler and Mangano, different PDF parametrisations can give very different result
- we will put this into practice and compute the K-factor for 5 different PDF choices at y=0. We will plot the energy-dependence of the K-factor for the PDFs:
  - CT14nlo_NF3
  - NNPDF31sx_nlo_as_0118
  - NNPDF31sx_nlonllx_as_0118
  - MRS(A')
  - MRS(G)
- in order to discriminate between the PDF choices we will use two different scale configurations:
  - $\mu_R = \mu_F = 2m_c = 3\text{GeV}$ - default scale choice
  - $\mu_R = m_c = 1.5\text{GeV}$, $\mu_F = 2m_c = 3\text{GeV}$
    - lower renormalisation choice leads to larger $\alpha_s \to$ real emission contributions become more important; the objective is to see the impact of the PDFs on the real corrections

# $K$-factor at $y = 0$ - $\mu_R = \mu_F = 2m_c = 3\text{GeV}$

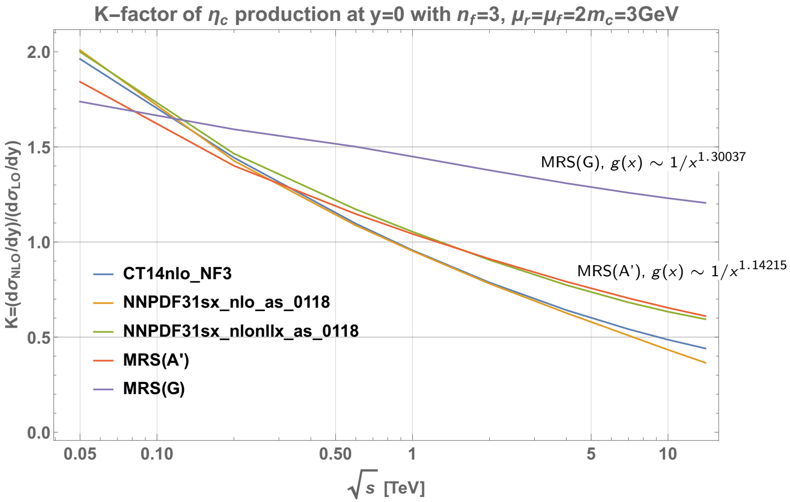


K-factor at y=0 as a function of energy and with different PDF choices. Default scale choice used $\mu_R = \mu_F = 2m_c = 3\text{GeV}$.

# $K$-factor at $y = 0$ - $\mu_R = m_c = 1.5\text{GeV}, \mu_F = 2m_c = 3\text{GeV}$

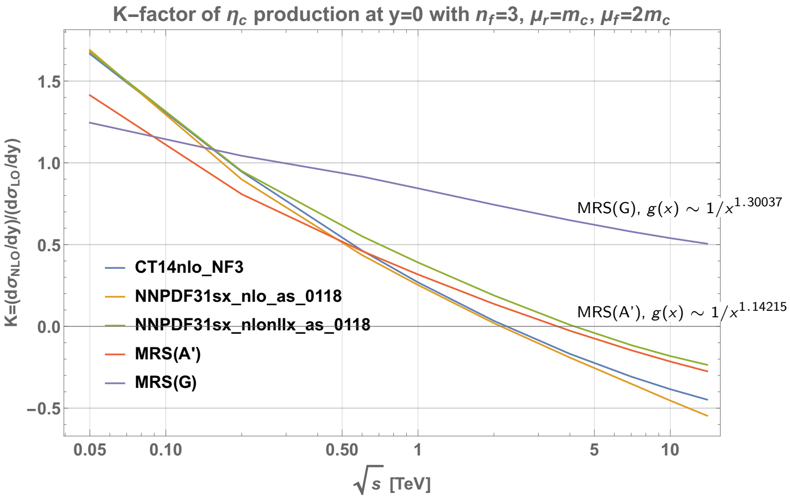


K-factor at y=0 as a function of energy and with different PDF choices. Alternative scale choice used $\mu_R = m_c = 1.5\text{GeV}$, $\mu_F = 2m_c = 3\text{GeV}$.

# NNPDF31 100 Replicas - Uncertainty of $K$-factor

- use {NNPDF31_nlo_as_0118, NNPDF31sx_nlo_as_0118, NNPDF31sx_nlonllx_as_0118} sets and run over 100 Replicas

# NNPDF31 100 Replicas - Uncertainty of $K$-factor

- use {NNPDF31_nlo_as_0118, NNPDF31sx_nlo_as_0118, NNPDF31sx_nlonllx_as_0118} sets and run over 100 Replicas
- difference between NNPDF31_nlo_as_0118 and NNPDF31sx_nlo_as_0118 is that the latter one with small x extension has been probed at a minimally lower scale $Q$ such that in the Replica generation the $2.7\mathrm{GeV}^2$ bin has been taken into account which turns out to be crucial

# NNPDF31 100 Replicas - Uncertainty of $K$-factor

- use {NNPDF31_nlo_as_0118, NNPDF31sx_nlo_as_0118, NNPDF31sx_nlonllx_as_0118} sets and run over 100 Replicas
- difference between NNPDF31_nlo_as_0118 and NNPDF31sx_nlo_as_0118 is that the latter one with small x extension has been probed at a minimally lower scale $Q$ such that in the Replica generation the $2.7\mathrm{GeV}^2$ bin has been taken into account which turns out to be crucial
- difference between NNPDF31sx_nlo_as_0118 and NNPDF31sx_nlonllx_as_0118 is that in the latter one NLL contributions are slowing down DGLAP equations, such that when it is fitted at higher $\mu_f$ to data, the back-evolution to initial scale will lead to steeper gluon parametrisations

# NNPDF31 100 Replicas - Uncertainty of $K$-factor

- use {NNPDF31_nlo_as_0118, NNPDF31sx_nlo_as_0118, NNPDF31sx_nlonllx_as_0118} sets and run over 100 Replicas
- difference between NNPDF31_nlo_as_0118 and NNPDF31sx_nlo_as_0118 is that the latter one with small x extension has been probed at a minimally lower scale $Q$ such that in the Replica generation the $2.7\mathrm{GeV}^2$ bin has been taken into account which turns out to be crucial
- difference between NNPDF31sx_nlo_as_0118 and NNPDF31sx_nlonllx_as_0118 is that in the latter one NLL contributions are slowing down DGLAP equations, such that when it is fitted at higher $\mu_f$ to data, the back-evolution to initial scale will lead to steeper gluon parametrisations
- expect very large $K$-factor uncertainty associated to normal NNPDF31 PDF choice and improvements for sx and sxNLL PDF choices

# NNPDF31 100 Replicas - Uncertainty of $K$-factor

- use {NNPDF31_nlo_as_0118, NNPDF31sx_nlo_as_0118, NNPDF31sx_nlonllx_as_0118} sets and run over 100 Replicas
- difference between NNPDF31_nlo_as_0118 and NNPDF31sx_nlo_as_0118 is that the latter one with small x extension has been probed at a minimally lower scale $Q$ such that in the Replica generation the $2.7\mathrm{GeV}^2$ bin has been taken into account which turns out to be crucial
- difference between NNPDF31sx_nlo_as_0118 and NNPDF31sx_nlonllx_as_0118 is that in the latter one NLL contributions are slowing down DGLAP equations, such that when it is fitted at higher $\mu_f$ to data, the back-evolution to initial scale will lead to steeper gluon parametrisations
- expect very large $K$-factor uncertainty associated to normal NNPDF31 PDF choice and improvements for sx and sxNLL PDF choices
- we will try with two different scale choices as before, set $y = 0$ and use $\sqrt{s} = 7\ \mathrm{TeV}$ and $14\ \mathrm{TeV}$

# $K$-factor results - $y = 0$ & $\sqrt{s} = 7$ TeV - 100 Replicas

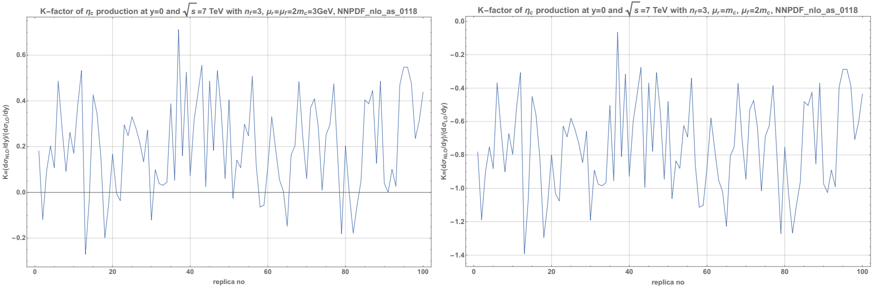


Figure: Strong variation of $K$-factor over replica number of NNPDF31_nlo_as_0118 (y=0, $\sqrt{s} = 7$ TeV, default/alternative scale choice)

default ($\mu_R = \mu_F = 2m_c = 3$GeV): $\rightarrow K = 0.2 \pm 0.2$
alternative ($\mu_R = m_c = 1.5$GeV, $\mu_F = 2m_c = 3$GeV): $\rightarrow K = -0.8 \pm 0.3$

# $K$-factor - default scale - summary so far

| | $\sqrt{s} = 7$ TeV | | | $\sqrt{s} = 14$ TeV |
|---|---|---|---|---|
| PDF choice | $y = 0$ | $y = 1$ | $y = 2$ | $y = 0$ |
| MRS(G) | 1.26 | 1.27 | 1.29 | 1.21 |
| MRS(A') | 0.70 | 0.72 | 0.76 | 0.61 |
| sxNLL-NNPDF31 (Replica) | 0.68±0.06 | 0.71±0.06 | 0.79±0.08 | 0.59±0.09 |
| CT14nlo_NF3 (central value) | 0.54 | 0.57 | 0.65 | 0.44 |
| sx-NNPDF31 (Replica) | 0.50±0.09 | 0.51±0.11 | 0.59±0.16 | 0.36±0.15 |
| normal-NNPDF31 (Replica) | 0.20±0.21 | 0.2±0.4 | 0.2±1.1 | −0.1±0.4 |

# Improve $K$-factor with constraints in Quarkonia

- can we improve the $K$-factor for NNPDF31 PDF sets by applying constraints?

# Improve $K$-factor with constraints in Quarkonia

- can we improve the $K$-factor for NNPDF31 PDF sets by applying constraints?
- strategy is to weight the Replicas based on their $K$-factors with a Gaussian distribution in a given set of results.

# Improve $K$-factor with constraints in Quarkonia

$$\chi_i^2 = (1 - K_i)^2, \tag{5}$$

$$w_i = \frac{e^{-\frac{\chi_i^2}{2\sigma^2}}}{\frac{1}{N_{\rm rep}} \sum_{j=1}^{N_{\rm rep}} e^{-\frac{\chi_j^2}{2\sigma^2}}} \tag{6}$$

with

$$\sigma = 0.3, \tag{7}$$

such that we are focusing on $K$-factors in the range $K = 1 \pm 0.3$

# Improve $K$-factor with constraints in Quarkonia

- can we improve the $K$-factor for NNPDF31 PDF sets by applying constraints?
- strategy is to weight the replicas based on their $K$-factors with a Gaussian distribution in a given set of results.
  $\rightarrow$ essentially assigning weights close to 0 for Replicas that gave negative $K$-factors

# Improve $K$-factor with constraints in Quarkonia

- can we improve the $K$-factor for NNPDF31 PDF sets by applying constraints?
- strategy is to weight the replicas based on their $K$-factors with a Gaussian distribution in a given set of results.
  $\rightarrow$ essentially assigning weights close to 0 for Replicas that gave negative $K$-factors
- we will use the results for $y = 0$ and $\sqrt{s} = 14$ TeV with default scale choice

# $K$-factor - default scale - updated summary

| | $\sqrt{s} = 7$ TeV | | | $\sqrt{s} = 14$ TeV |
|---|---|---|---|---|
| PDF choice | $y = 0$ | $y = 1$ | $y = 2$ | $y = 0$ |
| MRS(G) | 1.26 | 1.27 | 1.29 | 1.21 |
| sxNLL-NNPDF31 (Replica) **(reweighted)** | **0.70±0.06** | **0.73±0.06** | **0.81±0.08** | **0.62±0.08** |
| MRS(A') | 0.70 | 0.72 | 0.76 | 0.61 |
| sx-NNPDF31 (Replica) **(reweighted)** | **0.56±0.09** | **0.58±0.08** | **0.66±0.11** | **0.45±0.10** |
| CT14nlo_NF3 (central value) | 0.54 | 0.57 | 0.65 | 0.44 |
| normal-NNPDF31 (Replica) **(reweighted)** | **0.50±0.12** | **0.52±0.11** | **0.60±0.10** | **0.40±0.14** |

# CT14nlo 57 members - Uncertainty of $K$-factor

- CT14nlo pdf set has 1 central member ($f_0$) and 28 eigenset doublets ($f^+$ and $f^-$)

# CT14nlo 57 members - Uncertainty of $K$-factor

- CT14nlo pdf set has 1 central member ($f_0$) and 28 eigenset doublets ($f^+$ and $f^-$)
- the uncertainty is determined in the Hessian way w.r.t. the central value

# CT14nlo 57 members - Uncertainty of $K$-factor

- CT14nlo pdf set has 1 central member ($f_0$) and 28 eigenset doublets ($f^+$ and $f^-$)
- the uncertainty is determined in the Hessian way w.r.t. the central value
- generate Replicas $f_k$ from eigensets

$$f_k = f_0 + \sum_i^N \frac{f^+ - f^-}{2} R_{ki}, \tag{8}$$

where $R_{ki}$ are random numbers from a normalised Gaussian distribution with uniform variance centered at the origin

# CT14nlo 57 members - Uncertainty of $K$-factor

- CT14nlo pdf set has 1 central member ($f_0$) and 28 eigenset doublets ($f^+$ and $f^-$)
- the uncertainty is determined in the Hessian way w.r.t. the central value
- generate Replicas $f_k$ from eigensets

$$f_k = f_0 + \sum_i^N \frac{f^+ - f^-}{2} R_{ki}, \tag{8}$$

where $R_{ki}$ are random numbers from a normalised Gaussian distribution with uniform variance centered at the origin

- let's generate 10000 Replicas...

# CT14nlo 57 members - 10000 Replicas - Uncertainty of $K$-factor

- we generate 10000 Replicas from the 57 members and we obtain for the default and alternative scale choices the following,

| | $\sqrt{s} = 7$ TeV | | | $\sqrt{s} = 14$ TeV |
|---|---|---|---|---|
| PDF choice | $y = 0$ | $y = 1$ | $y = 2$ | $y = 0$ |
| CT14nlo (Replica) (*default*) | 0.45±0.28 | 0.4±0.9 | -1±127 | 0.3±0.5 |
| CT14nlo (Replica) (*alternative*) | -0.4±0.4 | -0.5±1.2 | -3±172 | -0.6±0.6 |

# CT14nlo 57 members - 10000 Replicas - Uncertainty of $K$-factor

- we generate 10000 Replicas from the 57 members and we obtain for the default and alternative scale choices the following,

| | $\sqrt{s} = 7$ TeV | | | $\sqrt{s} = 14$ TeV |
|---|---|---|---|---|
| PDF choice | $y = 0$ | $y = 1$ | $y = 2$ | $y = 0$ |
| CT14nlo (Replica) (*default*) | 0.45±0.28 | 0.4±0.9 | -1±127 | 0.3±0.5 |
| CT14nlo (Replica) (*alternative*) | -0.4±0.4 | -0.5±1.2 | -3±172 | -0.6±0.6 |

→ **need to re-weight Replicas!**

# CT14nlo 57 members - 10000 Replicas - Uncertainty of $K$-factor

- we will make a reweightment based on the results for $y = 2$ at the alternative scale to distinguish the good Replicas from the bad Replicas

# CT14nlo 57 members - 10000 Replicas - Uncertainty of $K$-factor

- we will make a reweightment based on the results for $y = 2$ at the alternative scale to distinguish the good Replicas from the bad Replicas
- as before we will use the Gaussian distribution to re-weigth with $\chi_i^2 = (1 - K_i)^2$ and $\sigma = 0.3$

# CT14nlo 57 members - 10000 Replicas - Uncertainty of $K$-factor

*default* scale choice,

| | $\sqrt{s} = 7$ TeV | | | $\sqrt{s} = 14$ TeV |
|---|---|---|---|---|
| PDF choice | $y = 0$ | $y = 1$ | $y = 2$ | $y = 0$ |
| CT14nlo (Replicas) *(default)* | 0.45±0.28 | 0.4±0.9 | -1±127 | 0.3±0.5 |
| CT14nlo (Replicas) *(default)* **(reweighted)** | **0.83±0.12** | **0.9±0.3** | **1.07±0.11** | **0.85±0.14** |

# $K$-factor at $y = 0$ - $\mu_R = \mu_F = 2m_c = 3\text{GeV}$

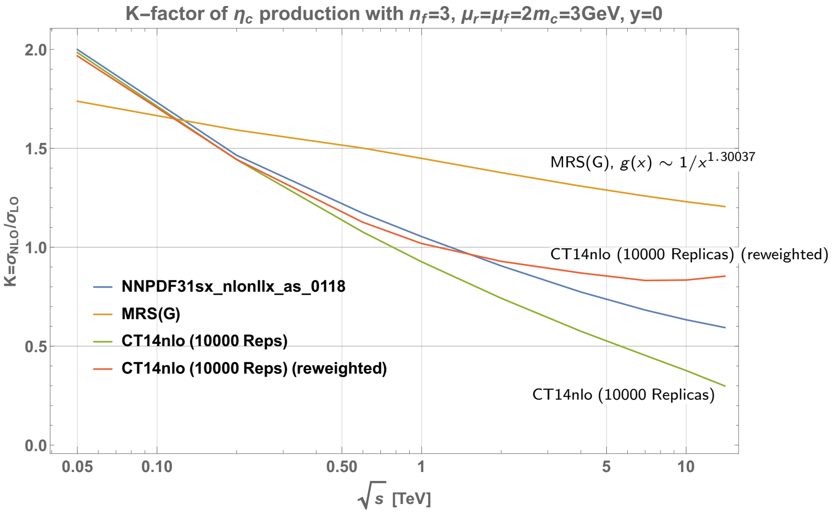


K-factor at y=0 as a function of energy and with different PDF choices. Default scale choice used $\mu_R = \mu_F = 2m_c = 3\text{GeV}$.

# CT14nlo 57 members - 10000 Replicas - Uncertainty of $K$-factor

*alternative* scale choice,

| | $\sqrt{s} = 7$ TeV | | | $\sqrt{s} = 14$ TeV |
|---|---|---|---|---|
| PDF choice | $y = 0$ | $y = 1$ | $y = 2$ | $y = 0$ |
| CT14nlo (Replicas) *(alternative)* | -0.4±0.4 | -0.5±1.2 | -3±172 | -0.6±0.6 |
| CT14nlo (Replicas) *(alternative)* **(reweighted)** | **0.09±0.16** | **0.2±0.4** | **0.41±0.15** | **0.12±0.19** |

# $K$-factor at $y = 0$ - $\mu_R = m_c = 1.5\text{GeV}, \mu_F = 2m_c = 3\text{GeV}$

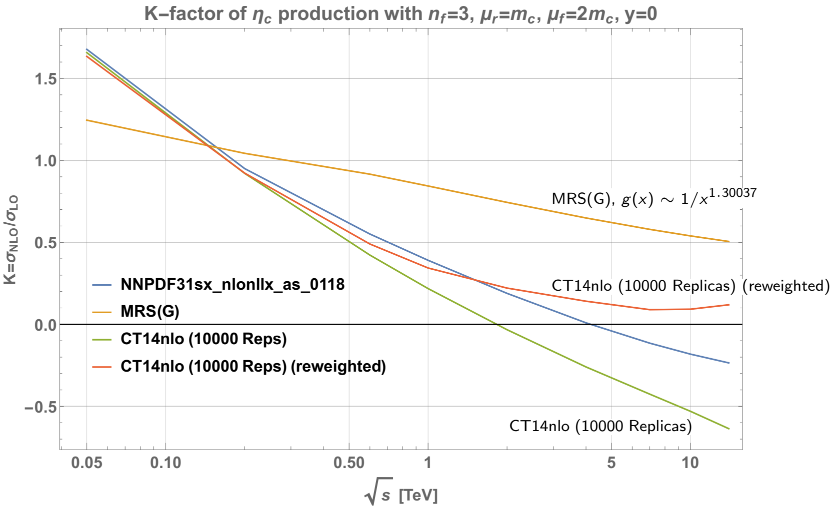


K-factor at y=0 as a function of energy and with different PDF choices. Alternative scale choice used $\mu_R = m_c = 1.5\text{GeV}$, $\mu_F = 2m_c = 3\text{GeV}$.

# next steps & further constraints on PDFs from Quarkonium Physics

- combine weighting by using results at different energies $\sqrt{s}$ and rapidities $y$

# next steps & further constraints on PDFs from Quarkonium Physics

- combine weighting by using results at different energies $\sqrt{s}$ and rapidities $y$
- further constraints for PDFs that we can take from Quarkonium Physics are

# next steps & further constraints on PDFs from Quarkonium Physics

- combine weighting by using results at different energies $\sqrt{s}$ and rapidities $y$
- further constraints for PDFs that we can take from Quarkonium Physics are
  - at fixed rapidity, the differential cross-section must increase with $\sqrt{s}$ energy

# next steps & further constraints on PDFs from Quarkonium Physics

- combine weighting by using results at different energies $\sqrt{s}$ and rapidities $y$
- further constraints for PDFs that we can take from Quarkonium Physics are
  - at fixed rapidity, the differential cross-section must increase with $\sqrt{s}$ energy
  - at fixed $\sqrt{s}$ energy, the differential cross-section should decrease with increasing rapidity; generically it should follow the shape of the leading order ($2 \to 1$ process)

# next steps & further constraints on PDFs from Quarkonium Physics

- combine weighting by using results at different energies $\sqrt{s}$ and rapidities $y$
- further constraints for PDFs that we can take from Quarkonium Physics are
  - at fixed rapidity, the differential cross-section must increase with $\sqrt{s}$ energy
  - at fixed $\sqrt{s}$ energy, the differential cross-section should decrease with increasing rapidity; generically it should follow the shape of the leading order ($2 \to 1$ process)

$\rightarrow$ work on-going

Thank you for attention!

# Backup

# TMD - Transverse Momentum Distribution

$$\sigma \propto H \times \mathcal{C}[f_1^g f_1^g] \tag{9}$$

$$\mathcal{C}[f_1^g f_1^g] = \int \frac{d^2\vec{b}_T}{(2\pi)^2} e^{i\vec{b}_T\cdot\vec{q}_T} \tilde{f}_1^g\left(x_1, \vec{b}_T; \zeta, \mu\right) \tilde{f}_1^g\left(x_2, \vec{b}_T; \zeta, \mu\right)$$

$$\tilde{f}_1^{g/A}\left(x, \vec{b}_T; \zeta, \mu\right) = \sum_{j=q,\bar{q},g} \int_x^1 \frac{d\tilde{x}}{\tilde{x}} \tilde{C}_{g/j}\left(\tilde{x}, \vec{b}_T; \zeta, \mu\right) f_{j/A}(x/\tilde{x}; \mu)$$

$$\tilde{C}_{g/g} = \delta(1-x) + \frac{\alpha_s}{2\pi}\left[C_A\delta(1-x)\left(-\frac{1}{2}L_T^2 + L_T \ln\frac{\mu^2}{\zeta} - \frac{\pi^2}{12}\right)\right.$$
$$\left. - L_T\left(P_{g/g} - \delta(1-x)\frac{\beta_0}{2}\right)\right]$$

$$\tilde{C}_{g/q} = \frac{\alpha_s}{2\pi}\left[-L_T P_{g/q} + C_F x\right]$$

$$L_T = \ln\frac{\mu^2 b_T^2}{4e^{-2\gamma_E}} \tag{10}$$

# TMD vs. collinear factorisation

- TMD factorisation is more universal than collinear factorisation

# TMD vs. collinear factorisation

- TMD factorisation is more universal than collinear factorisation
  - leading-order process plus virtual corrections are factorised into hard part $H$ (*process-dependent*)

# TMD vs. collinear factorisation

- TMD factorisation is more universal than collinear factorisation
  - leading-order process plus virtual corrections are factorised into hard part $H$ (*process-dependent*)
  - real and mixed real-virtual corrections are included inside the TMDPDFs (*process-independent*)

# TMD vs. collinear factorisation

- TMD factorisation is more universal than collinear factorisation
  - leading-order process plus virtual corrections are factorised into hard part $H$ (*process-dependent*)
  - real and mixed real-virtual corrections are included inside the TMDPDFs (*process-independent*)
- with positivity constraint $d\sigma/dy > 0$, we have that $\mathcal{C}[f_1^g f_1^g] > 0$ always (universal property)!

# TMD vs. collinear factorisation

- TMD factorisation is more universal than collinear factorisation
  - leading-order process plus virtual corrections are factorised into hard part $H$ (*process-dependent*)
  - real and mixed real-virtual corrections are included inside the TMDPDFs (*process-independent*)
- with positivity constraint $d\sigma/dy > 0$, we have that $\mathcal{C}[f_1^g f_1^g] > 0$ always (universal property)!
  - however we encounter at $\eta_c$ scales, that $\mathcal{C}[f_1^g f_1^g] < 0$

# TMD vs. collinear factorisation

- TMD factorisation is more universal than collinear factorisation
  - leading-order process plus virtual corrections are factorised into hard part $H$ (*process-dependent*)
  - real and mixed real-virtual corrections are included inside the TMDPDFs (*process-independent*)
- with positivity constraint $d\sigma/dy > 0$, we have that $\mathcal{C}[f_1^g f_1^g] > 0$ always (universal property)!
  - however we encounter at $\eta_c$ scales, that $\mathcal{C}[f_1^g f_1^g] < 0$

$\rightarrow$ constrain PDFs such that $\mathcal{C}[f_1^g f_1^g] > 0$ at $\eta_c$ scales

# TMD vs. collinear factorisation

- TMD factorisation is more universal than collinear factorisation
  - leading-order process plus virtual corrections are factorised into hard part $H$ (*process-dependent*)
  - real and mixed real-virtual corrections are included inside the TMDPDFs (*process-independent*)
- with positivity constraint $d\sigma/dy > 0$, we have that $\mathcal{C}[f_1^g f_1^g] > 0$ always (universal property)!
  - however we encounter at $\eta_c$ scales, that $\mathcal{C}[f_1^g f_1^g] < 0$

$\rightarrow$ constrain PDFs such that $\mathcal{C}[f_1^g f_1^g] > 0$ at $\eta_c$ scales

- re-weighting PDFs with similar criteria

# TMD vs. collinear factorisation

- TMD factorisation is more universal than collinear factorisation
  - leading-order process plus virtual corrections are factorised into hard part $H$ (*process-dependent*)
  - real and mixed real-virtual corrections are included inside the TMDPDFs (*process-independent*)
- with positivity constraint $d\sigma/dy > 0$, we have that $\mathcal{C}[f_1^g f_1^g] > 0$ always (universal property)!
  - however we encounter at $\eta_c$ scales, that $\mathcal{C}[f_1^g f_1^g] < 0$

  $\rightarrow$ constrain PDFs such that $\mathcal{C}[f_1^g f_1^g] > 0$ at $\eta_c$ scales
- re-weighting PDFs with similar criteria
- if the re-weighted Replicas obtained by imposing $d\sigma/dy > 0$ (+ good shape behaviour) in collinear factorisation more or less coincide with $\mathcal{C}[f_1^g f_1^g]$, this would mean that we are on the right track to use quarkonium as quantitative gluon probes

# TMD vs. collinear factorisation

- TMD factorisation is more universal than collinear factorisation
  - leading-order process plus virtual corrections are factorised into hard part $H$ (*process-dependent*)
  - real and mixed real-virtual corrections are included inside the TMDPDFs (*process-independent*)
- with positivity constraint $d\sigma/dy > 0$, we have that $\mathcal{C}[f_1^g f_1^g] > 0$ always (universal property)!
  - however we encounter at $\eta_c$ scales, that $\mathcal{C}[f_1^g f_1^g] < 0$

  $\rightarrow$ constrain PDFs such that $\mathcal{C}[f_1^g f_1^g] > 0$ at $\eta_c$ scales
- re-weighting PDFs with similar criteria
- if the re-weighted Replicas obtained by imposing $d\sigma/dy > 0$ ($+$ good shape behaviour) in collinear factorisation more or less coincide with $\mathcal{C}[f_1^g f_1^g]$, this would mean that we are on the right track to use quarkonium as quantitative gluon probes

  $\rightarrow$ work on-going

# Quarkonia - three different models

- Colour-Evaporation Model
  - quark and anti-quark colours are summed up at amplitude squared level (evaporation)
  - no spin-projection
- Colour-Octet Model
  - quark and anti-quark pair are in color-octet state
  - heavy quark spins projected on final bound state
  - higher Fock states in NRQCD, higher $v$-order
- **Colour-Singlet Model**
  - quark and anti-quark pair are in color-singlet state
  - heavy quark spins projected on final bound state
  - leading Fock state in NRQCD

gluon-gluon channel

$$\hat{\sigma}_{gg}(s,\hat{s},\mu_R,\mu_F) = \frac{\alpha_s^2(\mu_R)\pi^2}{96 m_c^5}|R(0)|^2\delta(1-z)$$
$$+\frac{\alpha_s^3(\mu_R)\pi}{1152 m_c^5}|R(0)|^2\left[\left(-44+7\pi^2+54\log\left(\frac{\mu_R^2}{\mu_F^2}\right)\right.\right.$$
$$\left.+72\log\left(1-\frac{4m_c^2}{s}\right)\left(\log\left(1-\frac{4m_c^2}{s}\right)-\log\left(\frac{\mu_F^2}{4m_c^2}\right)\right)\right)\delta(1-z)$$
$$+6\left(24\left(\frac{\log(1-z)}{1-z}\right)_\rho (1-(1-z)z)^2\right.$$
$$+12\left(\frac{1}{1-z}\right)_\rho \frac{\log(z)}{(1-z)(1+z)^3}\left(1-z^2\left(5+z\left(2+z+3z^3+2z^4\right)\right)\right)$$
$$-\left(\frac{1}{1-z}\right)_\rho \frac{1}{(1+z)^2}\left(12+z^2\left(23+z\left(24+2z+11z^3\right)\right)\right)$$
$$\left.\left.+12\left(1+z^3\right)^2\log\left(\frac{z\mu_F^2}{4m_c^2}\right)\right)\right], \text{ where } z=4m_c^2/\hat{s} \text{ and } \rho=4m_c^2/s \qquad (11)$$

quark-antiquark channel

$$\hat{\sigma}_{q\bar{q}}(\hat{s}, \mu_R) = \frac{16\alpha_s^3(\mu_R)\pi}{81 m_c} |R(0)|^2 \frac{(\hat{s} - 4m_c^2)}{\hat{s}^3} \tag{12}$$

quark-gluon channel

$$\begin{aligned}\hat{\sigma}_{qg}(\hat{s}, \mu_R, \mu_F) = \frac{\alpha_s^3(\mu_R)\pi}{72 m_c^5 \hat{s}^2} |R(0)|^2 \Big( & 8m_c^4 + 4m_c^2\hat{s} - \hat{s}^2 \\ & + 2\left(8m_c^4 - 4m_c^2\hat{s} + \hat{s}^2\right) \log\left(1 - \frac{4m_c^2}{\hat{s}}\right) \\ & + \hat{s}\left(-4m_c^2 + \hat{s}\right) \log\left(\frac{4m_c^2}{\hat{s}}\right) \\ & - \left(8m_c^4 - 4m_c^2\hat{s} + \hat{s}^2\right) \log\left(\frac{\mu_F^2}{\hat{s}}\right)\Big)\end{aligned} \tag{13}$$

# problem of negative cross-sections - $J/\psi$, ${}^1S_0^{[8]}$ at NLO

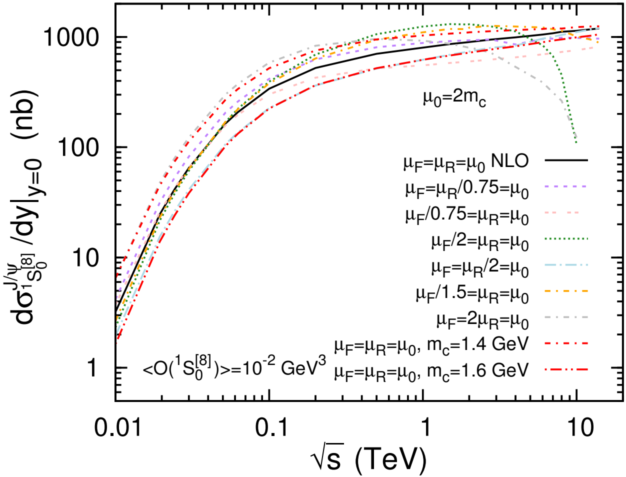


comparison of $J/\psi$ ${}^1S_0^{[8]}$ differential cross-section at NLO with different choices of $\mu_R$ and $\mu_F$ with CTEQ6M **[Y. Feng, J.-P. Lansberg, J.X. Wang, Eur.Phys.J. C75 (2015)]**

# Schuler 1994 - structure of partonic cross-section

- let's define $z = M^2/\hat{s}$ and $\tau_0 = M^2/s$
- LO partonic cross-section and virtual corrections ($2 \to 1$ process) have $\delta(1-z)$ function while real corrections ($2 \to 2$) are complicated functions of $z$
- negative contributions come from real corrections which have interference terms
- idea is to use simple toy-models for gluon PDFs and convolute with partonic cross-section; different $z$-terms will contribute differently at hadronic level

# Schuler 1994 - two toymodels - table partonic vs. hadronic

| $\hat{\sigma}_{gg}(z, M^2)$ | $xg(x) \to 1$ | $xg(x) \to 1/\sqrt{x}$ |
|---|---|---|
| | $\sigma_{pp}(\tau_0, M^2) \overset{\tau_0 \to 0}{\longrightarrow}$ | |
| $\delta(1-z)$ | $\ln\left(\frac{1}{\tau_0}\right)$ | $\frac{1}{\sqrt{\tau_0}} \ln\left(\frac{1}{\tau_0}\right)$ |
| $z^k$ | $\frac{1}{k} \ln\left(\frac{1}{\tau_0}\right)$ | $\frac{2}{(2k+1)\sqrt{\tau_0}} \ln\left(\frac{1}{\tau_0}\right)$ |
| $1$ | $\frac{1}{2} \ln^2\left(\frac{1}{\tau_0}\right)$ | $\frac{2}{\sqrt{\tau_0}} \ln\left(\frac{1}{\tau_0}\right)$ |
| $\ln^k\left(\frac{1}{z}\right)$ | $\frac{1}{(k+1)(k+2)} \ln^{k+2}\left(\frac{1}{\tau_0}\right)$ | $\frac{k!\,2^{k+1}}{\sqrt{\tau_0}} \ln\left(\frac{1}{\tau_0}\right)$ |

Asymptotic ($\tau_0 = M^2/s \to 0$) behaviour of the proton-proton or proton-antiproton cross section for various forms of the gluon-gluon subprocess ($z = M^2/\hat{s} = \tau_0/\tau$) and two extreme choices of the gluon distribution function. Taken from G. Schuler, Review, 1994

toymodel $g(x) = 1/x$: real corrections dominate at high energies;
toymodel $g(x) = 1/x^{1.5}$: all contributions have same energy scaling

# high energy behaviour - $\eta_c$ - partonic cross-section

partonic cross-section away from threshold, $z \to 0$

$$\lim_{z\to 0} \hat{\sigma}_{gg} = \frac{\alpha_s^3(\mu)\pi}{16 m_c^5} |R(0)|^2 \left( \log\left(\frac{4m_c^2}{\mu_F^2}\right) - 1 \right), \tag{14}$$

$$\lim_{z\to 0} \hat{\sigma}_{q\bar{q}} = 0, \tag{15}$$

$$\lim_{z\to 0} \hat{\sigma}_{qg} = \frac{\alpha_s^3(\mu)\pi}{72 m_c^5} |R(0)|^2 \left( \log\left(\frac{4m_c^2}{\mu_F^2}\right) - 1 \right) \tag{16}$$

# high energy behaviour - $\eta_c$ - partonic cross-section

partonic cross-section away from threshold, $z \to 0$

- $\mu_F = m_c$

$$\lim_{z\to 0} \hat{\sigma}_{gg} = \frac{\alpha_s^3(\mu)\pi}{16 m_c^5} |R(0)|^2 \left(\log(4) - 1\right) = 0.2 * \hat{\sigma}_{gg,LO}, \tag{17}$$

- $\mu_F = 2m_c$

$$\lim_{z\to 0} \hat{\sigma}_{gg} = \frac{\alpha_s^3(\mu)\pi}{16 m_c^5} |R(0)|^2 (-1) = -0.5 * \hat{\sigma}_{gg,LO}, \tag{18}$$

# hadronic cross-section - dependence on $\mu_F$

- toy model 1 PDF with $f_{g/p}(x) = 1/x$
  - dependence of hadronic cross-section on $\mu_F$
  - for $\mu_F > m_c$, hadronic cross-section is negative
  - for $\mu_F < m_c$, hadronic cross-section is positive
- toy model 2 PDF with $f_{g/p}(x) = 1/x^{1.5}$
  - weak dependence of hadronic cross-section on $\mu_F$
  - cross-section always positive (independent of choice of $\mu_F$)
- similar behaviour for $qg$ channel at high energies because of same asymptotic limit as in $gg$ channel apart from global factor

# high energy behaviour - partonic cross-section

- for non-steep PDF choices, the high-energy hadronic limit is governed by the high-energy partonic limit → strong dependence on factorisation scale $\mu_F$
- some values for $C_J$:
  - $C_J = 1$ for pseudo-scalar quarkonia $\eta_{c/b/t}$
  - $C_J = 43/27$ for $\chi_{c/b,0}$
  - $C_J = 53/36$ for $\chi_{c/b,2}$
  - $C_J = 11/12 + \log z$ for Higgs (in infinite-top quark mass limit)
- as an aside note, ratio between $qg$ and $gg$ channel in high-energy partonic limit is process-independent (same for Quarkonia and Higgs Physics)

$$\lim_{z \to 0} \frac{\hat{\sigma}_{qg}}{\hat{\sigma}_{gg}} = \frac{C_F}{2C_A} = \frac{2}{9} \tag{19}$$